

Contents lists available at ScienceDirect

Energy

journal homepage: www.elsevier.com/locate/energy



Facilely synthesized porous polymer as support of poly(ethyleneimine) for effective CO₂ capture



Maryam Irani, Andrew T. Jacobson, Khaled A.M. Gasem, Maohong Fan*

Departments of Chemical and Petroleum Engineering, University of Wyoming, Laramie, WY 82071, USA

ARTICLE INFO

Article history: Received 2 February 2018 Accepted 22 May 2018 Available online 22 May 2018

Keywords: CO₂ capture Porous polymer Adsorption Desorption Kinetics

ABSTRACT

In this work, an effective adsorbent (polyHIPE/PEI) was developed for use in CO₂ capture technologies. For this purpose, a porous polymer was prepared by high internal phase emulsion (HIPE) using 2-Ethylhexyl methacrylate (EHMA) and divinylbenzene (DVB). This prepared porous polymer (polyHIPE) was then used as a novel support for the wet impregnation of polyethylenimine (PEI), thus resulting in the polyHIPE/PEI adsorbent. The prepared adsorbent was characterized using Fourier transform infrared spectroscopy (FTIR), solid-state nuclear magnetic resonance (NMR) spectroscopy, scanning electron microscopy (SEM), thermogravimetric analysis (TGA), and Brunauer-Emmett-Teller (BET) surface area analyses. At the optimal PEI loading of 60 wt% on polyHIPE, the CO₂ sorption capacity reached 4 mmol CO₂/g-sorbent using 10 vol% CO₂ and 3 vol% H₂O in N₂ at 70 °C. Kinetic and thermodynamic adsorption studies showed that the activation energies for CO₂ adsorption and desorption of polyHIPE/PEI are 13.74 kJ/mol and 36.12 kJ/mol, respectively. These results indicate that CO₂ desorption using polyHIPE/PEI has the potential to reduce CO₂ capture cost due to the low activation energy and high CO₂ desorption rate. As such, polyHIPE/PEI constitutes an advantageous alternative to traditional methods in CO₂ capture from gas mixtures.

© 2018 Elsevier Ltd. All rights reserved.

1. Introduction

Carbon dioxide (CO₂) makes up a large portion of the greenhouse gases that contribute to climate changes and global warming. CO₂ capture and sequestration (CCS) technologies are effective options to reduce atmospheric CO₂ emissions [1,2]. In industry, CO₂ capture is typically performed using liquid amine absorption, which has several drawbacks such as solvent degradation, high regeneration energy requirements, and corrosion issues. Compared with traditional separation methods, the development of lower energy consumption processes has gained more attention [3]. Several authors reviewed comparison among CO₂ capture technologies comprehensively [4-6]. Solid adsorbents with a lower heat capacity than that of aqueous amine solutions have potential to reduce the energy required for regeneration. Among solid adsorbents, porous materials containing amine molecules have received more attention due to their energy saving advantages, including high adsorption capacity and high gas diffusion rates [3,6–8]. Accordingly, such cost-effective adsorbents with good performance should be considered to reduce the adverse effects of anthropogenic CO₂ emissions [8].

High internal phase emulsions (HIPEs) are emulsions with an internal phase (droplet) that makes up more than 74% of the total emulsion volume. The emulsion contains two immiscible phases with a surfactant that is not soluble in the internal phase [9,10]. HIPEs are able to be applied as templates to produce highly porous polymers that are known as polyHIPEs. These polyHIPEs are prepared by polymerization of the thin monomer layers that surround the internal-phase droplets of the HIPE solution. Subsequent removal of these droplets form a highly porous polymer [10]. Two emulsions types can be used to synthesize polyHIPEs, either oil-inwater (O/W) or water-in-oil (W/O). The formation of W/O HIPEs is accomplished by gradually adding an electrolyte aqueous solution to an oil phase/surfactant mixture under stirring [9]. PolyHIPEbased materials have been applied for a variety of applications, such as adsorbents [11], supports for organic synthesis [12,13], electrochemical sensors [14], controlled drug delivery systems [15], composites [16], and organic-inorganic hybrids [17,18].

An effective adsorbent for CO₂ capture has a maximum CO₂ adsorption capacity obtained at average flue gas temperatures of

^{*} Corresponding author. E-mail address: mfan@uwyo.edu (M. Fan).

 $40-70\,^{\circ}\text{C}$ and at 10-15% CO₂ concentration for flue gas from coal combustion or 5% CO₂ concentration for natural gas combustion flue streams [19,20].

Several porous polymers have been prepared and studied for CO₂ adsorption. Liu et al. [21] synthesized nanoporous poly(divinvlbenzene) (PDVB) under solvothermal conditions as a support to prepare PEI-impregnated PDVB sorbents. The adsorbent showed a maximum CO₂ capacity of 3.17 mmol/g with 15% CO₂/N₂ at 25 °C. Sung et al. [19] prepared a sorbent using impregnation of PEI into a porous aromatic framework (PAF-5) resulting in a maximum CO₂ capacity of 2.52 mmol/g with a PEI content of 40 wt % under a stream of 15% CO₂ in N₂ gas at 40 °C. Liu et al. [22] prepared a series of porous polymers using divinylbenzene (DVB) and ethylene glycol dimethyl acrylate (EGDMA), as a support for PEI loading via impregnation to prepare an adsorbent for CO₂ capture. The maximal CO₂ adsorption capacity was 3.28 mmol/g at 25 °C and 10 vol% CO₂ with a PEI loading of 30 wt%. Wang et al. [8] synthesized a hybrid porous adsorbent, where polyethylenimine (PEI)enveloped titanium dioxide nanoparticles (nano-TiO₂) were added into a styrene/divinylbenzene solution. The prepared sorbent showed a high CO₂ capacity of 4.5 mmol/g at 75 °C under a stream of 10% CO2 in N2 gas, however it required a high desorption temperature of 150 °C. In our previous work [23], a CO₂ adsorbent was prepared by impregnation of tetraethylenepentamine (TEPA) onto modified carbon nanotubes (CNTs). The maximum CO2 sorption capacity was 5 mmol CO₂/g-sorbent for 10 vol% CO₂ in N₂ along with 1 vol% H₂O at 60 °C. However the preparation of modified carbon nanotubes as support is quite complicated and uneconomical.

For industrial applications, an adsorbent for CO₂ capture should show fast adsorption and desorption kinetics, stable regeneration performance in several cycles, as well as have a low regeneration energy consumption to be considered an energy efficient adsorbent. The aim of this work is to prepare an efficient and costeffective adsorbent for CO₂ capture with high CO₂ sorption capacity, fast kinetics in CO₂ adsorption/desorption cycles, and a low energy consumption for regeneration. To achieve this aim, a porous polymer was synthesized by the simple emulsion polymerization of divinylbenzene (DVB) and 2-Ethylhexyl methacrylate (EHMA). This newly prepared porous polymer (PolyHIPE) was then used as a support for the impregnation of polyethylenimine (PEI). The resultant adsorbent (polyHIPE/PEI) was studied for its applicability in CO₂ capture. The effect of PEI content, adsorption temperature, and moisture content on the CO₂ adsorption capacity was studied. In addition, the CO2 adsorption kinetics and adsorbent regenerability was discussed.

2. Experimental

2.1. Preparation of adsorbents

The required chemicals, including 2-Ethylhexyl methacrylate (98%), divinylbenzene (technical grade, 80%), polyethylenimine, branched (average Mw~800), toluene (anhydrous, 99.8%), potassium persulfate (\geq 99.0%), potassium sulfate (\geq 99.0%) and span 80, were purchased from Sigma- Aldrich. However, the required gases in this work were supplied by United States Welding, Inc.

The first step in the adsorbent preparation is making the poly-HIPEs support. For this purpose, the oil phase was made up of 2-Ethylhexyl methacrylate (EHMA) (1.2 g), divinylbenzene (DVB) (2.8 g), toluene (4.5 mL), and span 80 (1.5 g). The aqueous phase consisting of DI water, potassium persulfate (0.15 g) and potassium sulfate (0.38 g) was added slowly to the oil phase under stirring. The volume fraction of the internal phase (aqueous) in the emulsion was 90%. The emulsion was then polymerized at 65 °C in an

oven for 24 h in a covered glass bottle. After polymerization the salts and remaining solvents were extracted using a Soxhlet apparatus with water followed by acetone for 24 h each. Finally the polyHIPEs were dried in an oven at 65 °C overnight. This prepared support, poly(DVB/EHMA), was termed polyHIPE throughout this work. The yield, Y, was calculated using Y= $(m_e/m_m)^*$ 100, where m_e is the weight of polyHIPE after the Soxhlet extraction, and m_m is the weight of monomers used in the polymerization process. The yield in this work was found to be ~85%. For this calculation it was assumed that the Soxhlet extraction removed all the surfactant, unreacted monomers, and salts from the polyHIPE.

The polyHIPE/PEI sorbents were prepared by wet impregnation. After PEI was dissolved in 20 mL of ethanol the polyHIPE powder was added to the solution and stirred for 24 h at room temperature. Next it was dried in an oven at 60 °C. The amount of PEI and polyHIPE added to the solution was chosen to produce polyHIPE/PEI adsorbents with PEI loadings of 20, 40, 50, 60, and 70 wt%. The weight percent of PEI in polyHIPE/PEI was based on the total weight of polyHIPE/PEI.

2.2. Characterization of sorbent

A Nicolet/iS50 spectroscope Fourier transform infrared spectrometer (FTIR) was applied with a frequency range of 4000–500 cm⁻¹ for characterization of the functionalities on the sorbent. A FEI Quanta 450 field emission scanning electron microscope with a Schottky field emission gun at an accelerating voltage of 5 kV was used to take scanning electron microscopy (SEM) images. A Quantachrome Autosorb IQ automated gas sorption analyzer was applied to gain BET (Brunauer-Emmett-Teller) surface area and BJH (Barrett-Joyner-Halenda) pore volume. A TA Instruments SDT Q600 under N₂ gas with a heating rate of 5 °C/min was used for thermogravimetric analysis (TGA). Solid-state ¹³C CP-MAS NMR spectra was obtained by a 400 MHz Bruker magnet with an INOVA UNITY console (Agilent). The NMR samples were analyzed in a 5 mm silicon nitride Varian rotor with a spinning speed of 10 KHz.

2.3. CO₂ sorption and regeneration experiments

Experiments were conducted by placing a quartz tube reactor containing 50 mg of polyHIPE/PEI mixed with 1000 mg of 30 mesh silica sand into a tube furnace. The adsorbent was mixed with sand to prevent an excessive pressure drop along the adsorber. For the adsorption experiments, 10 vol% CO_2 in N_2 was introduced to the reactor at a flow rate of 300 mL/min 3 vol% H_2O was inserted into this inlet gas stream using a syringe pump and vaporized before reaching the reactor using a heating tape. Each sorption test was continued until the outlet and inlet CO_2 concentrations were equal. CO_2 desorption was performed using the same experimental setup. For desorption at 90 °C, the carrier gas (99.9% N_2) flow rate was set at 300 mL/min. A schematic of the experimental set up used for CO_2 capture is shown in Fig. 1.

3. Results and discussions

3.1. Characterization

Solid-state nuclear magnetic resonance (NMR) spectroscopy was applied to study the chemical structure of polyHIPEs and the adsorption behavior of the CO₂ molecules on the adsorbent. The ¹³C NMR spectrum of the polyHIPE is shown in Fig. 2. In the aromatic region, the carbons in the benzene rings showed two peaks at 127.9 and 145.6 ppm. The two small peaks at 112.9 and 138.3 ppm are assigned to methylene and methine carbon atoms of unreacted

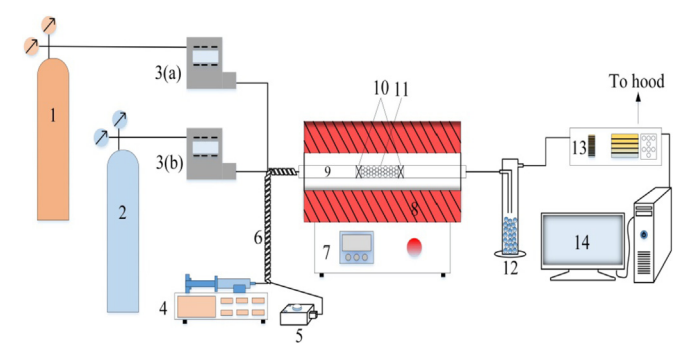


Fig. 1. Schematic diagram of CO₂ separation setup: 1, CO₂ cylinder; 2, N₂ cylinder; 3(a) CO₂ mass flow controller; 3(b), N₂ mass flow controller; 4, syringe pump; 5, heat tape temperature controller; 6, heat tape; 7, tube furnace temperature controller; 8, tube furnace; 9, quartz tube reactor; 10, quartz wool and notch block; 11, sorbent; 12, water removal unit; 13, gas analyzer; 14, data recording system.

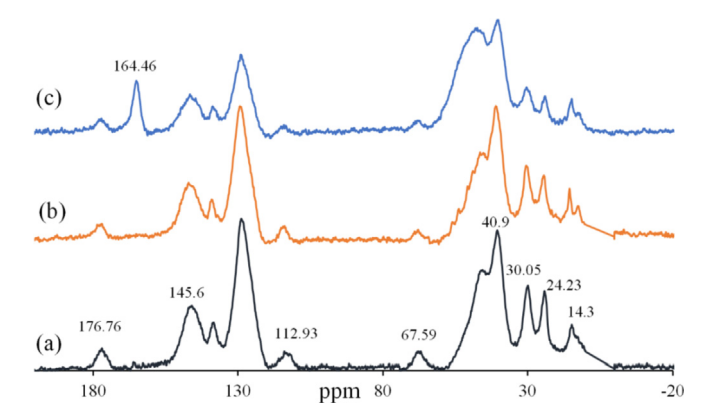


Fig. 2. 13 C CP-MAS NMR spectra of (a) polyHIPE, (b) polyHIPE/PEI (prior to contact CO₂), (c) polyHIPE/PEI after CO₂ adsorption (adsorption temperature; 70 °C in dry condition and CO₂ concentration; 10 vol% in N₂ gas).

vinyl groups [24]. The peaks that emerged at 176.76 and 67.59 ppm, correspond to C=O and C-O from 2-Ethylhexyl methacrylate. The multiple peaks at 14.3, 24.2, 30, and 40.9 ppm are attributed to the aliphatic carbons of polyHIPE. The suggested chemical structure of the synthesized support, polyHIPE, is shown in Fig. 3. Due to the presence of only two monomers in the polymerization process, the suggested structure is the most likely structure produced from polymerization.

¹³C NMR spectrums for the fresh and used adsorbent, polyHIPE/PEI, are depicted in Fig. 2 (b and c). Spectra for the fresh adsorbent includes a range of aliphatic carbons between 40 and 55 ppm, which is indicative of the polyethylenimine alkyl groups adjacent to amine groups [25]. These peaks show overlap with the peaks from the alkyl groups of the support (polyHIPE). After CO₂ adsorption, the used adsorbent shows a decrease in peak intensity of the alkyl

Fig. 3. Suggested chemical structure of the synthesized polyHIPE.

groups adjacent to amines groups $(40-55\,\mathrm{ppm})$, which may be a sign of the reaction between the amine groups and CO_2 occurring. The peak at 164.47 ppm in the used adsorbent spectra (Fig. 2c) is due to the presence of carbamate ions [25,26], which confirms that the reaction between CO_2 and the amine groups is chemisorption. In addition, the $^{13}\mathrm{C}$ NMR spectrum of the used adsorbent (Fig. 2c) shows no peak at 125 ppm which is assigned to physically adsorbed CO_2 [26]. This is additional evidence that the reaction between CO_2 and the adsorbent is chemisorption.

To confirm the incorporation of PEI into the porous polymer, the support (polyHIPE), polyethylenimine (PEI), and the adsorbent (polyHIPE/PEI) were characterized by FT-IR as shown in Fig. 4. The spectra of PEI (Fig. 4 a) shows double peaks at 3277 cm⁻¹ and 3355 cm⁻¹ which are attributed to the asymmetric and symmetric stretching vibrations of the N–H bond. The peak at 1590 cm⁻¹ is attributed to N–H bending vibrations from PEI, and the peak at 1044 cm⁻¹ corresponds to the stretching vibration of the C–N bond [21].

In the spectrum of polyHIPE the peaks at 2925 and 2856 cm⁻¹ correspond to the C–H stretching vibrations of the saturated aliphatic groups of polyHIPE. The characteristic peaks at 709 and 1600 cm⁻¹ correspond to benzene ring deformation vibrations and benzene ring stretching vibrations respectively [27]. The peak at 1725 cm⁻¹ is attributed to the carbonyl ester of EHMA from the support (polyHIPE). A very small peak at 1632 cm⁻¹ corresponds to unreacted vinyl groups. All the above characteristic peaks of PEI and polyHIPE can be seen in the spectrum of the polyHIPE/PEI (Fig. 4 c). This result confirms the incorporation of PEI in the support.

In addition, after incorporation of PEI in the support, the N–H bending vibration of PEI at 1590 cm⁻¹ from the PEI spectra (Fig. 4 a) is overlapped with the benzene ring vibration peak at 1600 cm⁻¹ from polyHIPE (Fig. 4 b). This resulted in a peak at 1587 cm⁻¹ in the spectra of polyHIPE/PEI (Fig. 4c). Also some of the characteristic peaks of the PEI and polyHIPE showed a slight shift in the spectra of polyHIPE/PEI. For example, the peak at 1725 cm⁻¹ from the polyHIPE spectra shifted to 1721 cm⁻¹ in the spectra of polyHIPE/PEI, suggesting electrostatic interactions between the carboxylic and amine functional groups of the support and PEI.

The BET surface area and the BJH pore volume for the support and the adsorbent are presented in Table 1. As shown, the surface area of polyHIPE is $201.1 \text{ m}^2/\text{g}$ with a pore volume of $0.805 \text{ cm}^3/\text{g}$. After a PEI loading of 60% into the polyHIPE, the surface area reduced by 90% to $20.03 \text{ m}^2/\text{g}$. This is another indication that PEI has been successfully loaded into the polyHIPE structure.

Scanning electron microscopy (SEM) images, Fig. 5, show the morphology of polyHIPE and polyHIPE/PEI. The polyHIPE images

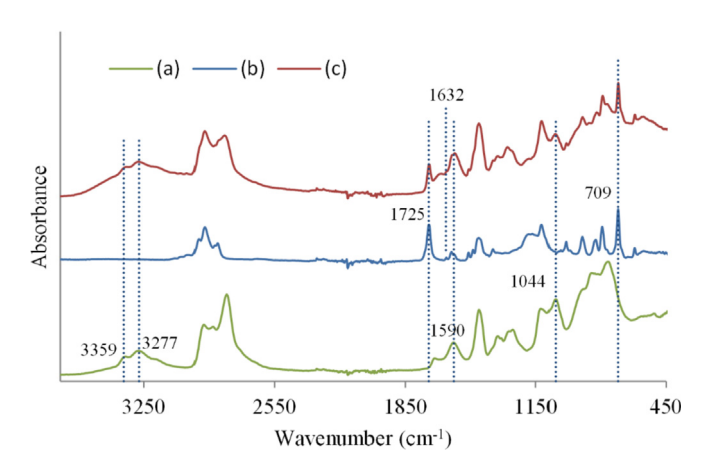


Fig. 4. FTIR spectra of (a) PEI (b) polyHIPE, and (c) polyHIPE/PEI.

 Table 1

 The texture properties of polyHIPE and polyHIPE/PEI with PEI loading of 60 wt%.

Sample	BET surface area (m ² /g)	BJH pore volume (cm³/g)
polyHIPE	201.1	0.805
polyHIPE/PEI	20.03	0.03

show a porous structure, while after introduction of PEI into the support, the polyHIPE/PEI images show a smooth surface with no obvious pores. These changes in the morphology of the support also confirm the incorporation of the PEI into the support which is consistent with the BET results (Table 1).

TGA weight loss curves of polyHIPE and polyHIPE/PEI are shown in Fig. 6. PolyHIPE (Fig. 6a) displayed a sharp mass loss of approximately 75 wt% from 280 to 430 °C, corresponding to the decomposition of polyHIPE. In the case of polyHIPE/PEI (Fig. 6b), a mass loss of approximately 3 wt% from 25 °C to 108 °C is due to the evaporation of adsorbed water. A second step of weight loss of around 21% between 107°C and 330°C is attributed to the decomposition of PEI located on the surface of the support. A third step of weight loss (41%) between 330 °C and 390 °C should be due to volatilization and decomposition of PEI located deep in the pores of the support as well as decomposition of the support. This was followed by a forth step of weight loss (28%) between 390 °C and 450 °C which may be attributed mostly to decomposition of the support and the loss of the residual PEI trapped in the support. Therefore, polyHIPE/PEI is thermally stable below 108 °C. In this work, this stability is appropriate for CO2 sorption at 70 °C and

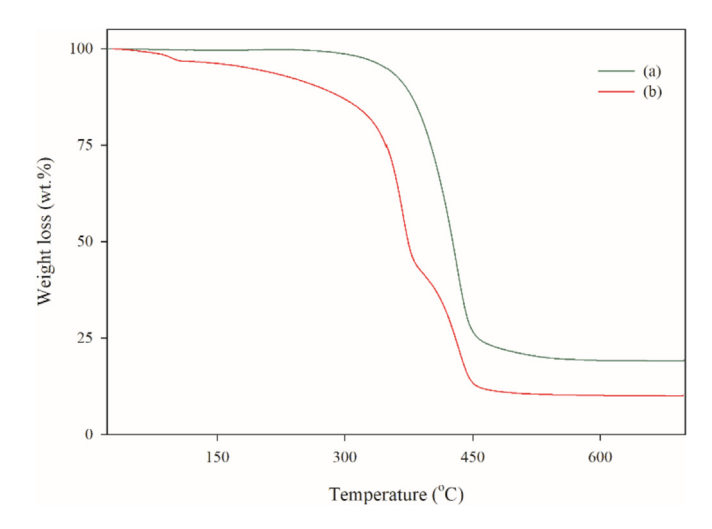


Fig. 6. TGA curves of (a) polyHIPE and (b) PolyHIP/PEI with PEI loading of 60 wt%.

desorption at 90 °C.

3.2. Effect of PEI loading on CO₂ sorption capacity

The availability of amine groups in amine-based sorbents is a key factor in CO₂ sorption because CO₂-amine interactions produce the desired adsorption. Therefore, the PEI loading amount is directly related to the CO₂ sorption capacity. Fig. 7 shows that

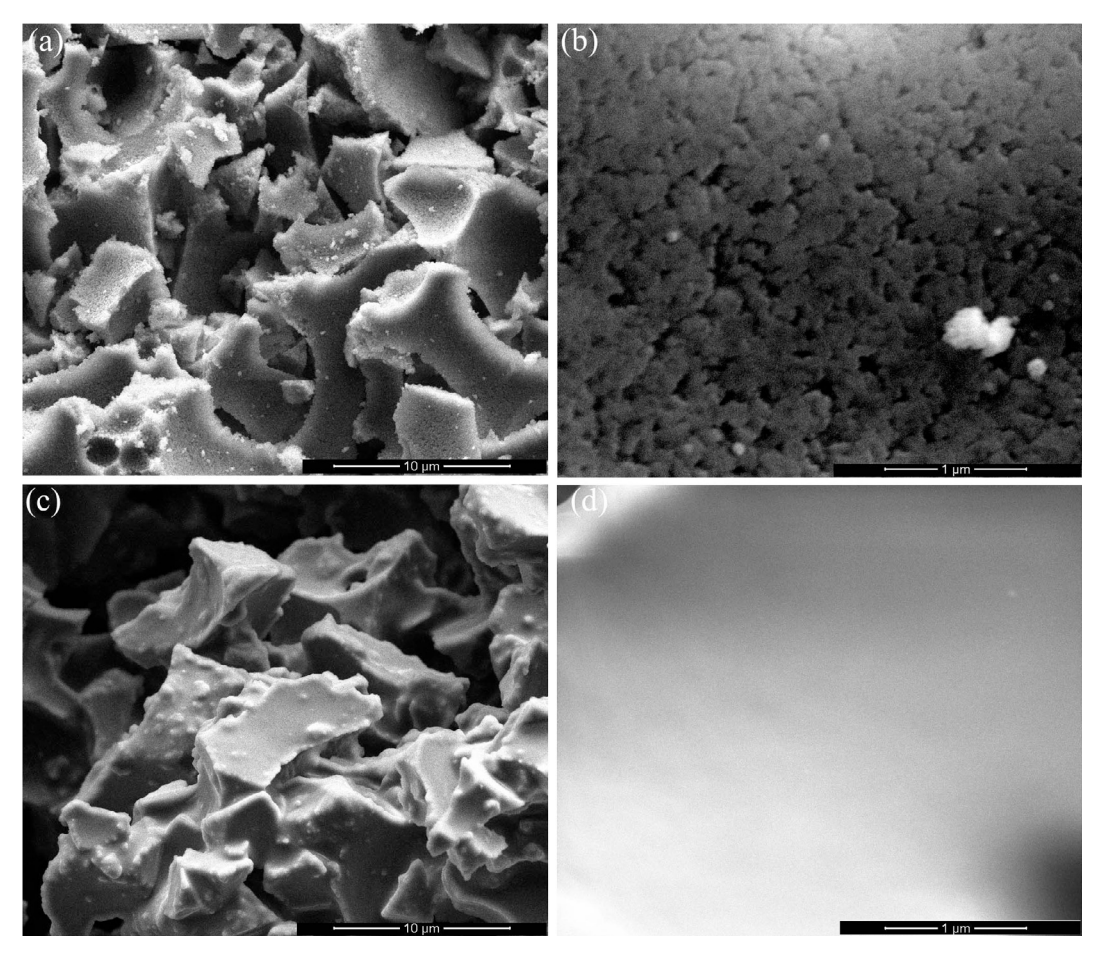


Fig. 5. SEM images of (a, b) polyHIPE and (c, d) polyHIPE/PEI.

increasing the PEI loading from 0 to 60 wt% results in increasing the CO_2 sorption capacity from 1.5 to 4 mmol/g. However, further increase in PEI loading to 70 wt% reduces the CO_2 sorption capacity. A decrease in the accessibility of amine groups from PEI agglomeration may explain this reduction in capacity.

It should be mentioned that initial tests along with previous works [23,28] were used to determine the optimal experimental starting points for the primary investigation. These starting points were applied in the final optimizations of PEI loading, temperature, and moisture content shown in Figs. 7–9.

3.3. Effect of sorption temperature on the CO₂ sorption capacity

In addition to PEI loading, sorption capacity is affected by the temperature of adsorption. PolyHIPE/PEI with a PEI loading of 60 wt % was selected for studying the effect of adsorption temperature on CO₂ capacity. Fig. 8 shows that the sorption capacity increased with an increasing temperature (25-70 °C). This suggests that beyond adsorption thermodynamics, some other effects are dominant and negate the expected decrease in adsorption. It has been suggested in other works [29,30] that the increased temperature may overcome the kinetic barrier as well as facilitate mass transfer of CO2 into the bulk of polymer. Further, the increasing temperature causes the expansion of PEI aggregates on the surface and within pores of adsorbent, thus providing more accessible active sites for adsorption. Nevertheless, at 80 °C, the equilibrium sorption capacity, as expected, decreases. Specifically, the adsorption thermodynamics overcome the kinetics involved, causing a decrease of CO_2 sorption capacity above 70 °C [29].

3.4. Effect of moisture addition

Studying the effect of moisture on CO_2 sorption capacity is important since CO_2 containing gases, such as flue gas, usually contain water vapor. Fig. 9 shows that the addition of 3 vol%

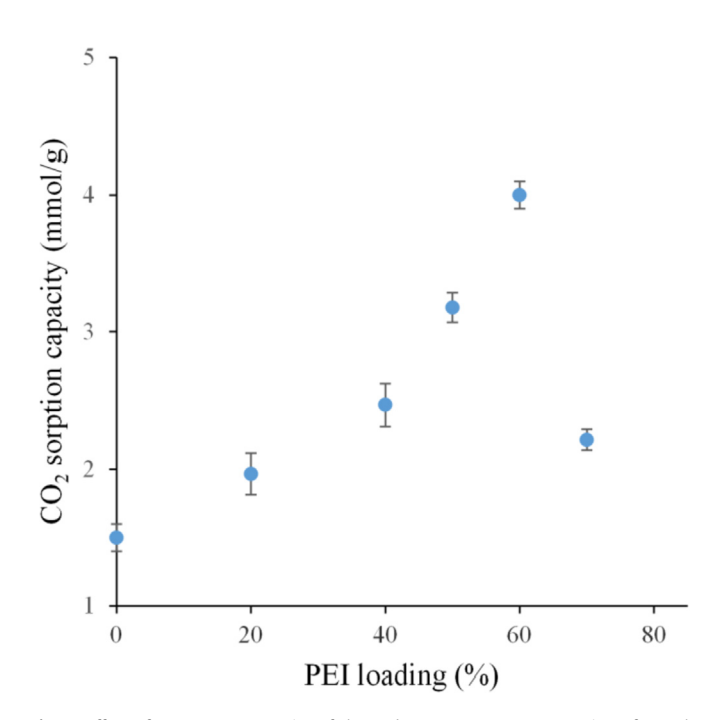


Fig. 7. Effect of PEI on CO_2 capacity of the sorbent at a CO_2 concentration of 10 vol% with the balance as N_2 gas, a gas flow rate of 300 mL/min, an adsorption temperature of $70 \, ^{\circ}\text{C}$, $3 \, \text{vol}\%$ moisture (H_2O) and $50 \, \text{mg}$ of sorbent. Error bars are the standard deviation of three experiments.

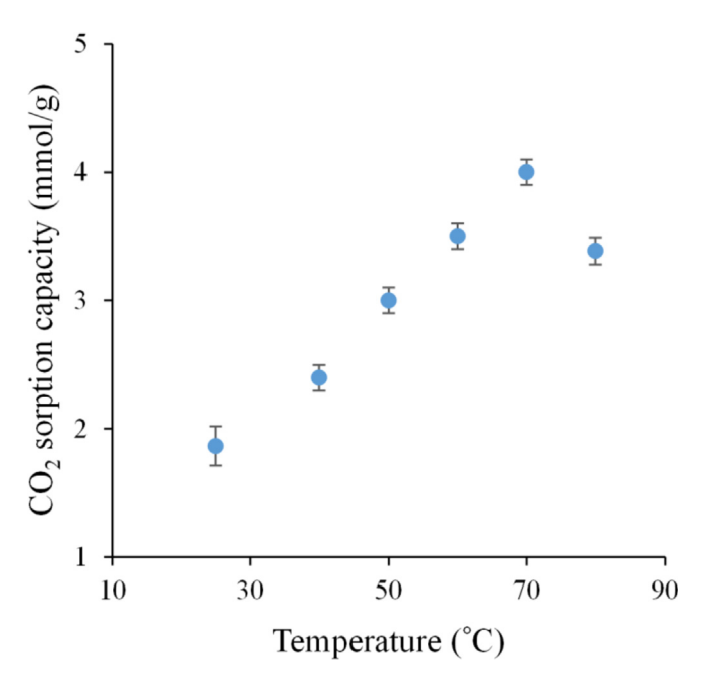


Fig. 8. The effect of temperature on CO_2 sorption capacity at a CO_2 concentration of 10 vol% with the balance as N_2 gas, a gas flow rate of 300 mL/min, a PEI loading of 60 wt %, 3 vol% moisture (H_2O) and 50 mg of sorbent. Error bars are the standard deviation of three experiments.

moisture increased CO₂ sorption capacity from 2.8 mmol/g to 4 mmol/g. However, the addition of more than 3 vol% decreased CO₂ adsorption capacity. This reduction may be due to water molecules competing with CO₂ for available adsorption sites [31]. The CO₂/amine reactions are different between wet and dry conditions. Dry conditions assist the formation of carbamates between two amine groups, while wet conditions make the formation of bicarbonates between one amine group and a CO₂ molecule [29,32].

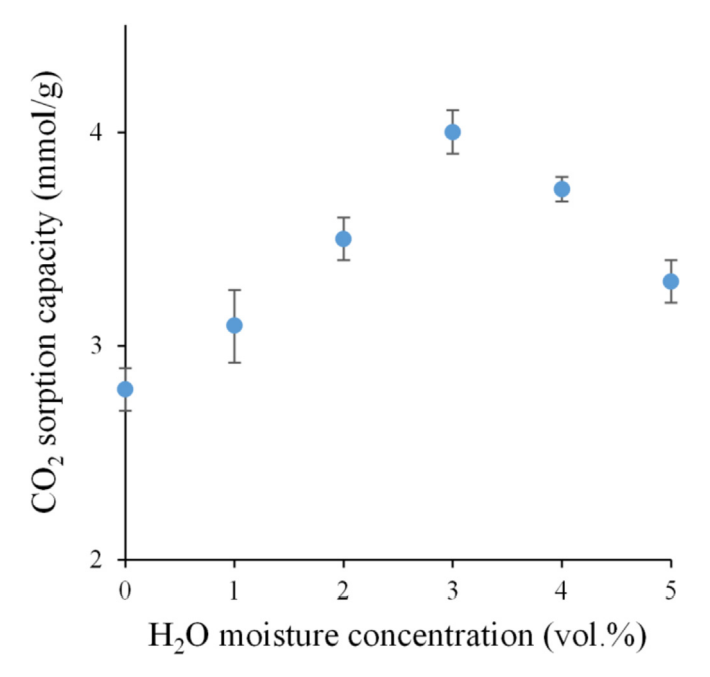


Fig. 9. The effect of moisture on CO_2 sorption capacity at a CO_2 concentration of 10 vol % with the balance as N_2 gas, a gas flow rate of 300 mL/min, an adsorption temperature of 70 °C, a PEI loading of 60 wt%, and 50 mg of sorbent. Error bars are the standard deviation of three experiments.

3.5. Adsorption/desorption kinetic models

To study the kinetics of CO₂ adsorption onto polyHIPE/PEI the following three models were considered:

3.5.1. Pseudo-first-order kinetic model

One of the most commonly used adsorption rate models is the pseudo-first-order kinetic model. It is given in Eq. (1) [7,33] below:

$$\frac{dq_t}{dt} = k_f(q_e - q_t) \tag{1}$$

where q_e and q_t (mmol/g) show the amount of CO_2 adsorbed at equilibrium and at a given time respectively, k_f (sec⁻¹) is the pseudo-first-order constant, and t is time (sec). After integration of Eq. (1) with the boundary conditions of t=0, $q_t=0$ and $t=\infty$, $q_t=q_e$, the resulting kinetic model is as follows:

$$q_t = q_e \left(1 - \exp\left(-k_f t \right) \right) \tag{2}$$

3.5.2. Pseudo-second order model

The mathematical model of the pseudo second order equation was first suggested by Blanchard et al. [34] to define the kinetics of heavy metal removal from water by zeolites. The model can be written as [33]:

$$\frac{dq_t}{dt} = k_s (q_e - q_t)^2 \tag{3}$$

where k_s (g mmol⁻¹ s⁻¹) is the second order kinetic constant. When Eq. (3) is integrated with the boundary conditions of t=0, $q_t=0$ and $t=\infty$, $q_t=q_e$, the adsorption capacity at a certain time leads to the following expression:

$$q_t = \frac{q_e^2 k_s t}{1 + q_e k_s t} \tag{4}$$

3.5.3. Langmuir adsorption model

The Langmuir adsorption model has been also used to study the adsorption kinetics of CO₂ onto adsorbents. The assumptions of Langmuir adsorption theory include equilibrium rates of adsorption and desorption on the surface are equivalent, a monolayer of the adsorbed molecules is formed on the surface, and the rate constants of adsorption and desorption are independent of the number of adsorbed molecules on the surface [35,36].

The CO_2 adsorption rate on the surface is as shown below [35,36]:

$$\frac{d\theta}{dt} = k_{aL}C_0(1-\theta) \tag{5}$$

where θ shows the fraction of surface coverage, and k_{aL} (s⁻¹atm⁻¹) is the adsorption rate constant, and C_0 depicts concentration or partial pressure of CO_2 in the gas.

Data from Table 2 shows that the equilibrium CO_2 capacity as predicted by the pseudo-first order and Langmuir models are in agreement with the experimental data, but the pseudo-second order model overestimated the CO_2 capacity at equilibrium. Comparison of the kinetic model representations of the experimental CO_2 adsorption data at $40\,^{\circ}C$ and $70\,^{\circ}C$ are shown in Fig. 10.

Data from the pseudo-first order and Langmuir models (Table 2) show that the kinetic rate constant increases with increasing adsorption temperature up to 70 °C. Further increases (80 °C)

Table 2Kinetic model parameters for CO₂ adsorption on polyHIPE/PEI.

Model	Parameters	Tempera	ture (°C)			
		40	50	60	70	80
Pseudo-f	first order					
	q_e	2.37	2.96	3.46	4.00	3.38
	k_f	0.012	0.012	0.016	0.018	0.014
	R^2	0.9975	0.9955	0.9987	0.9986	0.9989
Pseudo-s	Pseudo-second order					
	q_e	2.44	3.10	3.6	4.22	3.5
	k_s	0.0091	0.0068	0.0055	0.0072	0.0049
	R^2	0.9929	0.9968	0.9953	0.992	0.9952
Langmui	r					
	q_e	2.36	2.96	3.45	4.00	3.37
	k_{aL}	0.149	0.165	0.196	0.218	0.175
	R^2	0.9976	0.9956	0.9987	0.9986	0.9989

 $k_f[=] s^{-1}, k_s[=] g mmol^{-1} s^{-1}, k_{aL}[=] s^{-1} atm^{-1}, q_e[=] mmol/g.$

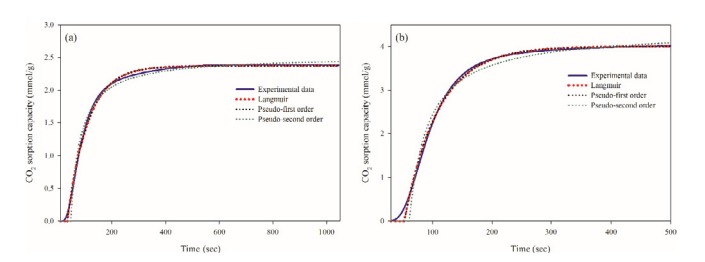


Fig. 10. CO₂ adsorption kinetics on polyHIPE/PEI at (a) 40 °C and (b) 70 °C.

resulted in a decrease of the kinetic rate constant. This is in agreement with previously discussed results in section (3.3). The decrease in the kinetic rate constant from 70 $^{\circ}\text{C}$ to 80 $^{\circ}\text{C}$ is evidence that the process thermodynamics surpass the kinetics. This outcome is likely due to the exothermic nature of the process at these conditions.

At lower temperatures the adsorption step is slower than that of higher temperatures. For example, at 40 °C the adsorption equilibrium was achieved at ~17 min, while at 70 °C the equilibrium was achieved within ~8 min. It is suggested that the faster adsorption kinetics with temperature may be caused by faster diffusion of CO_2 molecules at high temperatures. In support of this explanation, it has been reported that fast kinetics of the reaction between CO_2 molecules and amino groups is best achieved at high temperatures [37].

Based on the above modeling results, the Langmuir adsorption model was chosen for further study. The CO_2 desorption rate from the surface using the Langmuir model is written as

$$\frac{d\theta}{dt} = -k_{dL}\theta\tag{6}$$

where k_{dL} is the desorption rate constant. Combining the Langmuir adsorption rate and desorption rate, and making use of the following maximum capacity relationship

$$q = q_{\text{max}}\theta \tag{7}$$

produces the following equations upon integration:

$$q = q_{\text{max}}[1 - \exp(-k_{aL}C_0t)] \tag{8}$$

$$q = q_{\text{max}} \exp(-k_{dL}t) \tag{9}$$

which expresses surface coverage in terms of capacity q, and maximum capacity (q_{max}) [35,36].

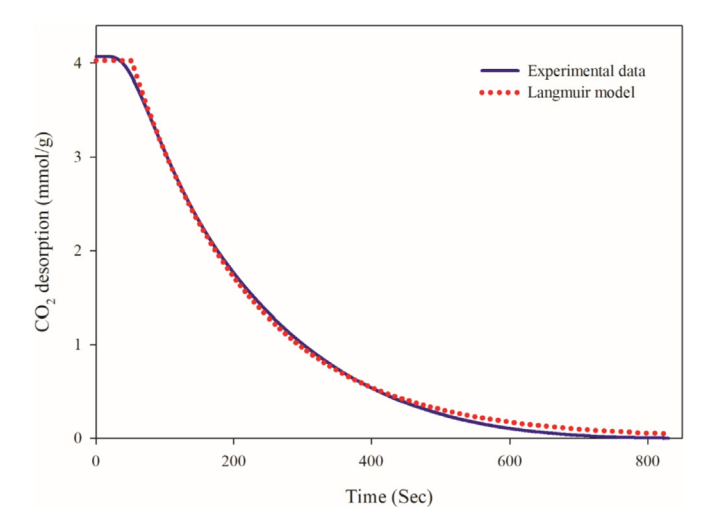


Fig. 11. The CO_2 desorption curve polyHIPE/PEI (blue lines: experimental data, red lines: Langmuir model fit to obtain k_d) [CO_2 concentration: 10 vol%; balance gas: N_2 ; gas flow rate: $300 \, \text{mL/min}$; H_2O : $3 \, \text{vol}$ %; adsorption temperature: $70 \, ^{\circ}C$; PEI loading: $60 \, \text{wt}$ %; desorption temperature: $90 \, ^{\circ}C$; desorption carrier gas: N_2 with a flow rate of $300 \, \text{mL/min}$; weight of sorbent: $50 \, \text{mg}$].

Adsorption measurements are used to determine values of k_{aL} and k_{dL} by regressing Eqs. (8) and (9), respectively. The kinetic rate constants of adsorption and desorption from the above mentioned kinetic models were obtained using the solver function in Microsoft Excel. A representative fit for the desorption data is shown in Fig. 11. A quality fit was obtained with correlation coefficients of 0.998 for the desorption curve.

The adsorption and desorption kinetics were also studied using the Arrhenius equation as written below [38].

$$\ln k = -\frac{E_a}{RT} + \ln A \tag{10}$$

which involves the reaction rate constant (k), the activation energy (E_a) , the reaction temperature (T) in kelvin (K), the molar gas constant (R), and the frequency factor (A). The kinetic rate constants of adsorption and desorption calculated from Eqs. (8) and (9) were used in Eq. (10) to calculate the activation energy (E_a) of adsorption and desorption, respectively. The activation energy and frequency factor are obtained by plotting $\ln k$ versus 1/T with a linear fit, as depicted in Fig. 12.

The desorption of CO $_2$ from the sorbent was completed at a low temperature (90 °C) within a short time (~13 min). The polyHIPE/PEI CO $_2$ adsorption and desorption E $_a$ values of 13.74 kJ/mol and 36.12 kJ/mol, respectively, are low. These data show that the CO $_2$ adsorption rate and desorption rate are high, which means the

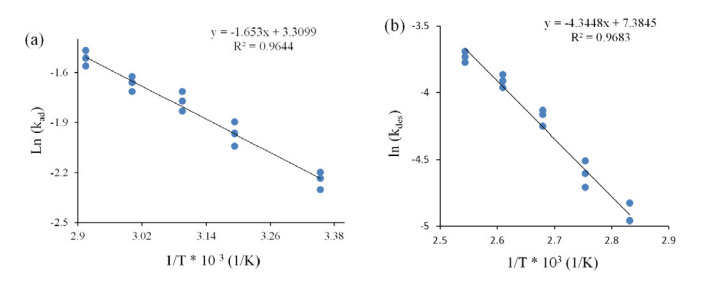


Fig. 12. Arrhenius plots of polyHIPE/PEI for adsorption (a) and desorption (b). [CO₂ concentration: 10 vol%; balance gas: N₂; gas flow rate: 300 mL/min; H₂O: 3 vol%; PEI loading: 60 wt%; desorption carrier gas: N₂ with a flow rate of 300 mL/min; weight of sorbent: 50 mg].

necessary amount of sorbent is reduced, and in turn, the capture cost of CO₂ is lowered. Moreover, a decrease in operating cost can be expected from a lower amount of adsorbent due to a reduction of temperature change and pressure drop in the flue gas [38].

In comparison with literature Ea values of aqueous amine-based absorption (40–50 kJ/mol), published solid adsorption E_a values are mostly lower [7,39]. The obtained activation energy in this work for desorption is comparable to the reported results of other solid amine-based sorbents. For example, Liu et al. [7] reported CO₂ desorption activation energy between 41 and 46 kJ/mol with a CO₂ capacity of around 4 mmol/g under a stream of 2 vol % CO₂ gas at 16 °C. In their study, they impregnated tetraethylenepentamine (TEPA) in industrial grade multiwalled carbon nanotubes (IG-MWCNTs). In our previous work [23], a CO₂ sorbent using immobilized tetraethylenepentamine (TEPA) onto modified carbon nanotubes (MCNTs) was prepared. The CO₂ sorption capacity was 5 mmolg for 10 vol% CO₂ in N₂ along with 1 vol% H₂O at 60 °C. Using the Arrhenius equation the activation energies for CO₂ adsorption and desorption of MCNTs/TEPA were 16.2 kJ/mol and 39.9 kJ/mol, respectively.

Hence, the low energy requirement and the relatively high CO_2 sorption capacity of polyHIPE/PEI make it an effective CO_2 adsorbent.

The heat of the reaction can be calculated as follows [38].

$$\Delta H = E_{a,ads} - E_{a,des} \tag{11}$$

Where ΔH is the heat of the reaction, and $E_{a,ads}$ and $E_{a,des}$ are the activation energies of adsorption and desorption, respectively, calculated from the Arrhenius equation (Eq. (10)). ΔH was calculated to be -22.38 kJ/mol for polyHIPE/PEI. The negative value of ΔH confirms that the sorption of CO_2 onto polyHIPE/PEI is an exothermic process.

3.6. Regenerability

From an industrial point of view, an effective adsorbent should be regenerable through several sorption—desorption cycles. In this work, the study of sorbent regenerability was tested in 10 sorption-desorption cycles. The results from Fig. 13 show that after 10 cycles of CO₂ adsorption/desorption, the CO₂ adsorption capacity slightly

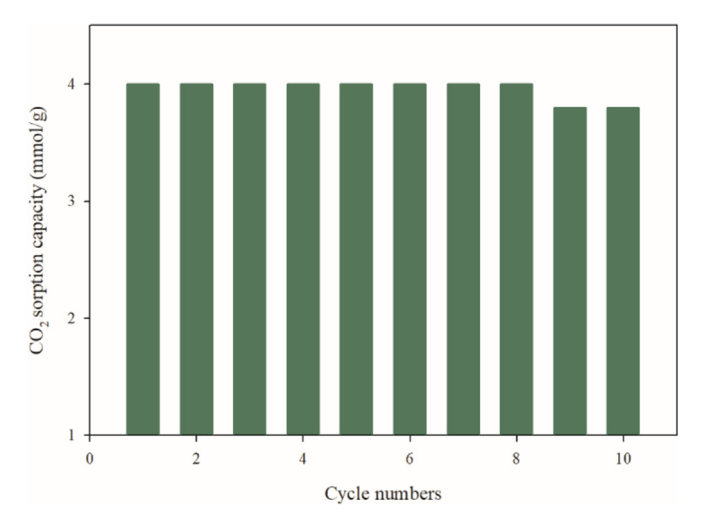


Fig. 13. Cyclic CO_2 sorption and desorption [sorption conditions: CO_2 concentration, 10 vol%; gas flow rate, 300 mL/min; H_2O : 3 vol%; sorption temperature, $70 \,^{\circ}\text{C}$; PEI loading: 60 wt%; desorption conditions: N_2 flow rate, 300 mL/min; desorption temperature, $90 \,^{\circ}\text{C}$; weight of sorbent: 50 mg].

reduced by about 5% (4 mmol/g to 3.8 mmol/g). The degradation and evaporation of small PEI molecules can be attributed to this loss of CO_2 sorption capacity.

4. Conclusions

A polyHIPE was synthesized as a support for preparation of an adsorbent with PEI via impregnation. An optimal PEI loading of 60 wt% achieved the maximal CO_2 sorption capacity of 4 mmol/g for a gas mixture containing 10 vol% CO_2 in N_2 with 3 vol% H_2O . Thermal stability studies show that polyHIPE/PEI is stable below 110 °C. PolyHIPE/PEI kinetic results of CO_2 adsorption and desorption indicate a low energy requirement and a short-time cycle for regeneration; therefore, polyHIPE/PEI can significantly reduce the overall cost of CO_2 capture.

The next step in reaching industrial application is through pilotscale tests in sorbent capacity and sorbent stability. Further study into the reaction kinetics and thermodynamics with the variation of CO2 partial pressure in the system is recommended.

Acknowledgment

Authors would like to thank National Science Foundation (NSF OIA-1632899) for providing funding for the research presented. Authors would like also to thank Dr. Bimala Lama from University of Colorado Boulder for ¹³C-NMR tests.

Nomenclature

Α	Frequency factor, for desorption (s^{-1}) and for adsorption
	$(s^{-1}atm^{-1})$
C_0	Partial pressure of CO ₂ in the gas (atm)
Ea	Activation energy (kJ/mol)
k_{aL}	Longmuir adsorption rate constant $(s^{-1}atm^{-1})$
k_{dL}	Longmuir desorption rate constant (s^{-1})
k_f	Pseudo-first-order constant (s ⁻¹)
k_s	Pseudo-second order kinetic constant(g mmol ⁻¹ s ⁻¹)
q_e	Amount of CO ₂ adsorbed at equilibrium(mmol/g)
q_t	Amount of CO ₂ adsorbed at a given time(mmol/g)
R	molar gas constant (kJ K ⁻¹ mol ⁻¹)
t	Time (s)
T	Temperature (°C)
vol%	Volume percentage

Greek symbols

θ	Fraction of surface coverage
ΔΗ	Heat of the reaction (kJ/mol)

Abbreviations

BET	Brunauer-Emmett-Teller surface area analyses
BIH	Barrett-Joyner-Halenda pore volume

DVB Divinylbenzene

EHMA 2-Ethylhexyl methacrylate

FTIR Fourier transform infrared spectroscopy

HIPEs High internal phase emulsions NMR Nuclear magnetic resonance

PEI Polyethylenimine

Sec Second

SEM Scanning electron microscopy TGA Thermogravimetric analysis

References

- [2] Huang Y-F, Chiueh P-T, Shih C-H, Lo S-L, Sun L, Zhong Y, Qiu C. Microwave pyrolysis of rice straw to produce biochar as an adsorbent for CO₂ capture. Energy 2015;84:75–82.
- [3] Liu Y, Lin X, Wu X, Liu M, Shi R, Yu X. Pentaethylenehexamine loaded SBA-16 for CO₂ capture from simulated flue gas. Powder Technol 2017;318:186–92.
- [4] Mondal MK, Balsora HK, Varshney P. Progress and trends in CO₂ capture/separation technologies: a review. Energy 2012;46:431–41.
- [5] Blomen E, Hendriks C, Neele F. Capture technologies: improvements and promising developments. Energy Procedia 2009;1:1505–12.
 [6] Kenarsari SD, Yang D, Jiang G, Zhang S, Wang J, Russell AG, Wei Q, Fan M.
- [6] Kenarsari SD, Yang D, Jiang G, Zhang S, Wang J, Russell AG, Wei Q, Fan M. Review of recent advances in carbon dioxide separation and capture. RSC Adv 2013;3:22739–73.
- [7] Liu Q, Shi J, Zheng S, Tao M, He Y, Shi Y. Kinetics studies of CO₂ adsorption/ desorption on amine-functionalized multiwalled carbon nanotubes. Ind Eng Chem Res 2014;53:11677–83.
- [8] Wang Q, Ma H, Chen J, Du Z, Mi J. Interfacial control of polyHIPE with nano-TiO₂ particles and polyethylenimine toward actual application in CO₂ capture. J. Environ. Chem. Eng 2017;5:2807–14.
- [9] He H, Li W, Lamson M, Zhong M, Konkolewicz D, Hui CM, Yaccato K, Rappold T, Sugar G, David NE, Damodaran K, Natesakhawat S, Nulwala H, Matyjaszewski K. Porous polymers prepared via high internal phase emulsion polymerization for reversible CO₂ capture. Polymer 2014;55:385–94.
- [10] Barbetta A, Cameron NR, Cooper SJ. High internal phase emulsions (HIPEs) containing divinylbenzene and 4-vinylbenzyl chloride and the morphology of the resulting PolyHIPE materials. Chem Commun 2000:221–2.
- [11] Pulko I, Kolar M, Krajnc P. Atrazine removal by covalent bonding to piperazine functionalized PolyHIPEs. Sci Total Environ 2007;386:114–23.
- [12] Dong X, Wang Y, Huang Y, Liu J, Jing X. Preparation of GSH-functionalized porous dextran for the selective binding of GST by high internal phase emulsion (HIPE) polymerization. J Mater Chem 2011;21:16147–52.
- [13] Li W, Zhang W, Dong X, Yan L, Qi R, Wang W, Xie Z, Jing X. Porous heterogeneous organic photocatalyst prepared by HIPE polymerization for oxidation of sulfides under visible light. J Mater Chem 2012;22:17445–8.
- [14] Zhao C, Danish E, Cameron NR, Kataky R. Emulsion-templated porous materials (PolyHIPEs) for selective ion and molecular recognition and transport: applications in electrochemical sensing. J Mater Chem 2007;17:2446–53.
- [15] Lim H, Kassim A, Huang N, Khiewc P, Chiu W. Three-dimensional flower-like brushite crystals prepared from high internal phase emulsion for drug delivery application. Colloids Surf, A 2009;345:211–8.
- [16] Normatov J, Silverstein MS. Silsesquioxane-cross-linked porous nanocomposites synthesized within high internal phase emulsions. Macromolecules 2007;40:8329–35.
- [17] Silverstein MS, Tai H, Sergienko A, Lumelsky Y, Pavlovsky S. PolyHIPE: IPNs, hybrids, nanoscale porosity, silica monoliths and ICP-based sensors. Polymer 2005;46:6682–94.
- [18] Normatov J, Silverstein MS. Porous interpenetrating network hybrids synthesized within high internal phase emulsions. Polymer 2007;48:6648–55.
- [19] Sung S, Suh MP. Highly efficient carbon dioxide capture with a porous organic polymer impregnated with polyethylenimine. J. Mater. Chem.A 2014;2: 13245–9.
- [20] McDonald TM, Mason JA, Kong X, Bloch ED, Gygi D, Dani A, Crocellà V, Giordanino F, Odoh SO, Drisdell WS, Vlaisavljevich B, Dzubak AL, Poloni R, Schnell SK, Planas N, Lee K, Pascal T, Wan LF, Prendergast D, Neaton JB, Smit B, Kortright JB, Gagliardi L, Bordiga S, Reimer JA, Long JR. Cooperative insertion of CO₂ in diamine-appended metal-organic frameworks. Nature 2015;519: 303.
- [21] Liu F, Huang K, Yoo C-J, Okonkwo C, Tao D-J, Jones CW, Dai S. Facilely synthesized meso-macroporous polymer as support of poly(ethyleneimine) for highly efficient and selective capture of CO₂. Chem Eng J 2017;314:466–76.
- [22] Liu F, Chen S, Gao Y. Synthesis of porous polymer based solid amine adsorbent: effect of pore size and amine loading on CO2 adsorption. J Colloid Interface Sci 2017;506:236–44.
- [23] Irani M, Jacobson AT, Gasem KAM, Fan M. Modified carbon nanotubes/tetraethylenepentamine for CO₂ capture. Fuel 2017;206:10–8.
- [24] Barbetta A, Cameron NR. Morphology and surface area of emulsion-derived (PolyHIPE) solid foams prepared with oil-phase soluble porogenic Solvents: three-component surfactant system. Macromolecules 2004;37:3202—13.
- [25] Drage TC, Arenillas A, Smith KM, Snape CE. Thermal stability of polyethylenimine based carbon dioxide adsorbents and its influence on selection of regeneration strategies. Microporous Mesoporous Mater 2008;116: 504–12.
- [26] Pinto ML, Mafra L, Guil JM, Pires J, Rocha J. Adsorption and activation of CO₂ by amine-modified nanoporous materials studied by solid-state NMR and ¹³CO₂ adsorption. Chem Mater 2011;23:1387–95.
- [27] Li T, Liu H, Zeng L, Yang S, Li Z, Zhang J, Zhou X. Macroporous magnetic poly(styrene-divinylbenzene) nanocomposites prepared viamagnetite nanoparticles-stabilized high internal phase emulsions. J Mater Chem 2011;21:12865–72.
- [28] Irani M, Gasem KAM, Dutcher B, Fan M. CO₂ capture using nanoporous TiO(OH)₂/tetraethylenepentamine. Fuel 2016;183:601–8.
- [29] Wang W, Xiao J, Wei X, Ding J, Wang X, Song C. Development of a new clay supported polyethylenimine composite for CO₂ capture. Appl Energy 2014;113:334–41.
- [30] Ma X, Wang X, Song C. "Molecular basket" sorbents for separation of CO_2 and H_2S from various gas streams. J Am Chem Soc 2009;131:5777–83.

- [31] Mohammad SA, Gasem KAM. Multiphase analysis for high-pressure adsorption of CO2/water mixtures on wet coals. Energy Fuels 2012;26:3470–80.
- [32] He L, Fan M, Dutcher B, Cui S, X-d Shen, Kong Y, Russell AG, McCurdy P. Dynamic separation of ultradilute CO₂ with a nanoporous amine-based sorbent. Chem Eng J 2012;189–190:13–23.
- [33] Álvarez-Gutiérrez N, Gil MV, Rubiera F, Pevida C. Kinetics of CO₂ adsorption on cherry stone-based carbons in CO₂/CH₄ separations. Chem Eng J 2017;307: 249–57.
- [34] Blanchard G, Maunaye M, Martin G. Removal of heavy metals from waters by means of natural zeolites. Water Res 1984;18:1501–7.
- [35] Chen M-S, Fan H-F, Lin K-C. Kinetic and thermodynamic investigation of Rhodamine B adsorption at solid/solvent interfaces by use of evanescent-wave cavity ring-down spectroscopy. Anal Chem 2009;82:868–77.
- [36] Zhou X, Yi H, Tang X, Deng H, Liu H. Thermodynamics for the adsorption of SO₂, NO and CO₂ from flue gas on activated carbon fiber. Chem Eng J 2012;200:399–404.
- [37] Liu Q, Shi J, Wang Q, Tao M, He Y, Shi Y. Carbon dioxide capture with polyethylenimine-functionalized industrial-grade multiwalled carbon nanotubes. Ind Eng Chem Res 2014;53:17468–75.
- [38] Dutcher B, Fan M, Leonard B, Dyar MD, Tang J, Speicher EA, Liu P, Zhang Y. Use of nanoporous FeOOH as a catalytic support for NaHCO₃ decomposition aimed at reduction of energy requirement of Na₂CO₃/NaHCO₃ based CO₂ separation technology. J Phys Chem C 2011;115:15532—44.
- [39] Paul S, Ghoshal AK, Mandal B. Absorption of carbon dioxide into aqueous solutions of 2-piperidineethanol: kinetics analysis. Ind Eng Chem Res 2009;48:1414–9.